Local Thermal Stress Analysis at the Bond Area

OPTI 523 Project Report Tianquan Su

1 Introduction

These days, adhesives are widely used in mirror mounting instead of fasteners. Bonded structures are often lighter in weight, lower in cost, and easier to assemble than those mechanical methods.

Most adhesives have pretty high thermal expansion coefficient (CTE) that can be ten times as large as the CTEs of glasses and metals. This mismatch in CTEs will introduce a thermal stress at the bond area when temperature changes. Because of the low modulus of elasticity (E) of adhesives and the thin layer geometry that adhesives are applied in practical usage, the thermal stress caused by adhesives is usually ignorable compare with the stress caused by different CTEs of the bonded parts. But the effects of the adhesives do exist, and can become considerable when other effects have been well controlled. Experiences from optical engineers and opticians show that local fringes can be seen localizing at the bond area due to temperature change. The phenomenon shows that the thermal stress cause by adhesives is able to deflect the mirror surface. This will cause a problem in high requirement system. So it will be helpful to study how the stress develops at the bond area, how it affects the mirror surface, and how it related to the material properties and geometry of adhesives.

My project tries to show theoretically and experimentally what will happen in real cemented joints using Milbond and GE RTV 566 as a function of cement thickness. The data sheets of these two adhesives are attached in appendix. Finite element analysis (FEA) and experiment test are used to study the adhesive thermal effect. The deflection of the mirror surface is parametrically (with charts) related to the properties and geometry of the adhesives.

2 Theory

Materials expand or contract with changing temperature. (Usually expansion happens when temperature goes up and vice versa.) Imagine a beam with length L1 under Temperature T1 expands to L2 when temperature goes up to T2, as shown in Figure 1:

Figure 1: Thermal expansion. T1<T2

This phenomenon is described by:

$$L_2 - L_1 = \alpha L(T_2 - T_1)$$

$$\Delta L = \alpha L \Delta T$$

$$\varepsilon = \frac{\Delta L}{L} = \alpha \Delta T$$

Where α is the coefficient of thermal expansion (CTE); ε is the thermal strain.

When two materials with different CTEs are bonded together, for example adhesive and glass, the strain will be forced to be the same (assume the bond does not fail). But the different expansion tendency will cause a stress at the interface.

Consider the adhesive joint connecting two parts. The adhesive usually has much higher CTE than the connected parts, which makes the adhesive tends to expand more than the jointed parts. The interior part of the adhesive bond is constrained by the adhesive around it, so it can only expand in the direction normal to the bond interface which is not constrained. The difference of expansion between adhesive and jointed parts is small at this area. But the adhesive near the edge is free to bulge laterally, where the adhesive tend to expand more differently to the jointed parts. Thus, the distribution of expansion tendency will introduce a stress distribution. The effect is illustrated in Figure2:

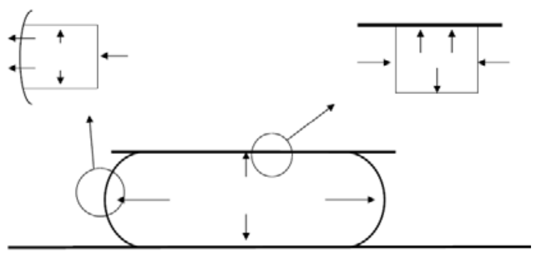

Figure 2: Thermal expansion of adhesive bond

The results should match with this effect.

3 Approach

3.1 Finite Element Analysis (FEA)

The FEA software, COSMOSWorks (embedded in SolidWorks), was used to analyze the thermal effect at the bond area. The model was built according to the hardware of the experimental test. Two pieces of B270 glass window were bonded by adhesives. By bonding two substrates made of the same material, the effect of the CTE differences between adherents was removed. The glass windows were 0.9 mm thick, and 50 mm in diameter. The properties of B270 are shown in appendix.

The adhesives chosen were Milbond from Summers Optics and GE RTV 566 in respective models. The corresponding properties are shown in appendix. In the model, the bonds had 25 mm diameter, which was comparatively large so as to show the effect better. The thicknesses of the adhesive were set as variable to see how the thickness related to the thermal effect.

Because of the cyclical symmetry of the model, only a portion of it (a 10˚ fan shape model) is made. With certain restraints set, COSMOSWorks is able to treat the fan model as a disc. This model considerably reduced the calculation and illustrated the stress distribution clearer. The model is shown as follows:

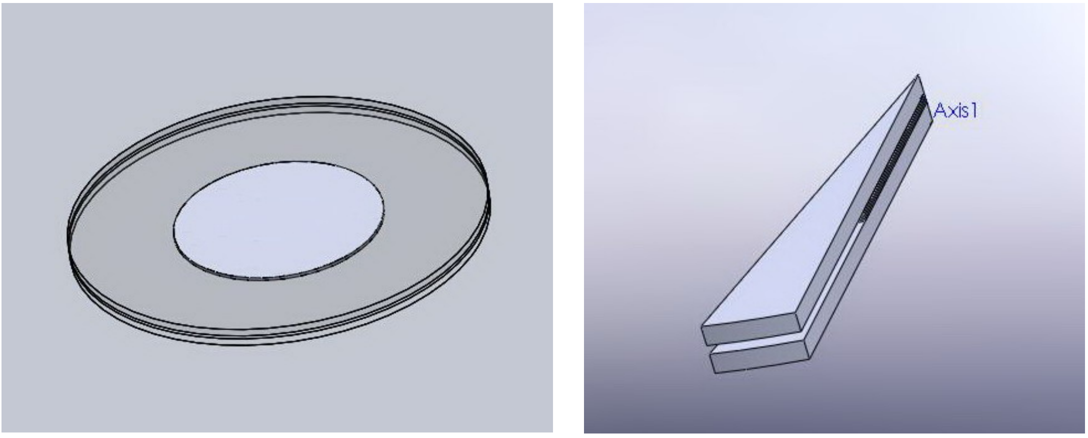

Figure 3: FEA model. The whole sample looks like the picture on the left; the fan model is shown on the right

During the analysis, certain boundary conditions (for example the cyclical symmetry) and proper restraints (imitating the real situation) were set. The original temperature was set at room temperature (24.85˚C). Then the changed temperature was set in the "restraint" section.

3.2 Experimental Test

The materials used in experiment were the same to the model. For each sample, two pieces of B270 glass window with 0.9 mm thickness and 50 mm diameter were bonded together with Milbond or RTV 566. Figure 4 illustrates the configuration of the sample.

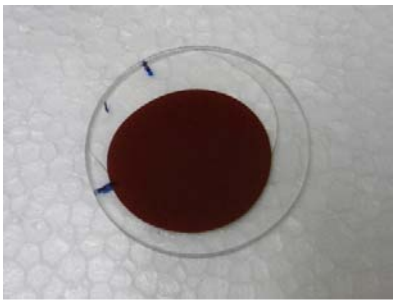

Figure 4: Sample to be test. It consists of two pieces of B270 window bonded with Milbond

Seven samples were made for the test. All these samples were made of two B270 windows with 50 mm diameter and 0.9 mm thickness. The geometries of the bonds are shown in Table 1:

Table 1: Geometry of bond samples

Sample #	Adhesive material	Adhesive thickness	Bond diameter
S 1	Milbond	0.4 mm	35 mm
S 2	Milbond	0.19 mm	30 mm
S 3	Milbond	0.6 mm	35 mm
S 4	Milbond	0.4 mm	10 mm
S 5	GE RTV 566	0.75 mm	40 mm
S 6	GE RTV 566	0.9 mm	38 mm
S 7	GE RTV 566	0.75 mm	15 mm

The thicknesses of the bonds were controlled with plastic shims. Three tiny pieces of shims with certain thickness were placed between the glasses when making the bond. They were removed after the adhesive had cured. The Milbond samples were cured at 160˚F for 3 hours, as the instruction showed. RTV 566 samples were cured at room temperature for 7 days.

The window surfaces were tested with interferometer (Zygo phase shifting). To reduce the disturbing reflection from other glass-air interfaces, BK7 matching oil is injected into the gap between the bonded windows, as one can see in Figure 4. The data sheet of the BK7 matching oil is attached in appendix.

The configuration of the test devices are shown as follows:

Figure 5: Device configuration. It consists of a Fizeau interferometer, a fold mirror, a temperature chamber and a thermometer

This set of equipments included a Zygo phase-shifting interferometer (with HeNe laser), a fold mirror, a temperature chamber, a stage and a thermometer. The light path was folded to remove the effect of gravity.

The stage was put up in a semi-kinematic way to ensure the repeatability of the test. All plates and stages are stacked up with three-point contact. The position of stages and plates are all fully constrained.

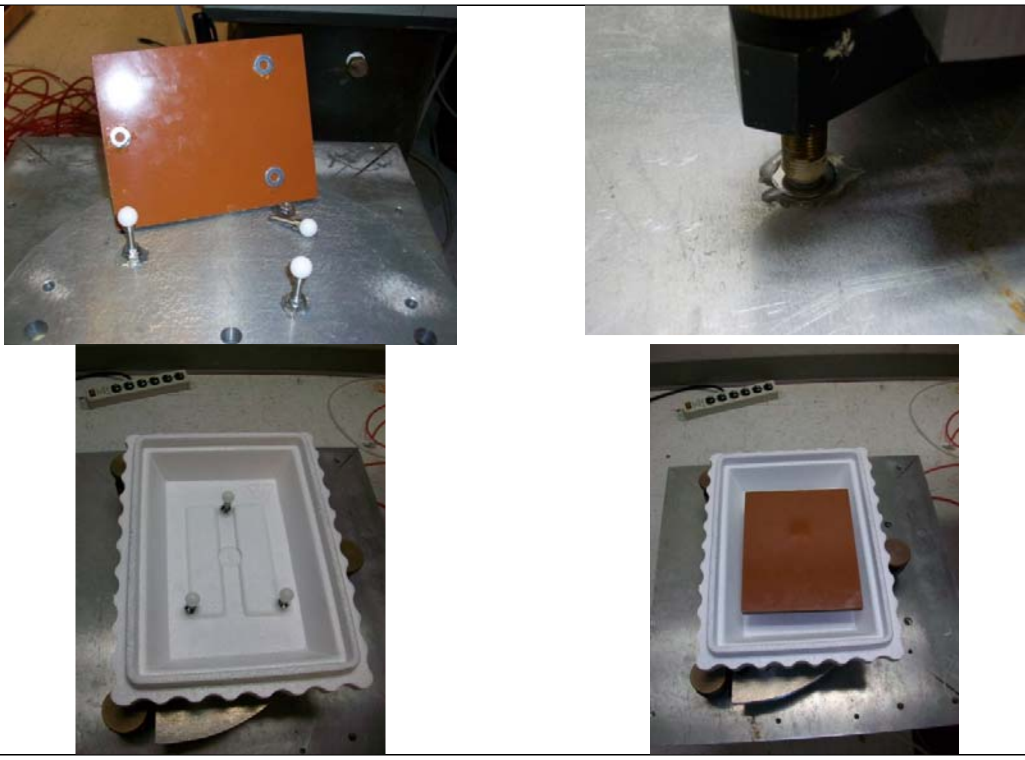

Figure 6: Some details of stage setting

Three poles with nylon balls went through the beach cooler lid to support a plastic plate where the samples were placed during test. This made sure that the support was stiff and would not be influenced by the compliance of the foam. The lid of the beach cooler was taped down to the stage. The holes where the poles go through were filled with cotton balls to reduce the heat lost.

A hole was cut on the top of the temperature chamber, and a double-layer window was attached by RTV. See Figure 7. The double-layer window design was to reduce the heat lost as well as the deflection caused by the thermal gradient inside and outside the chamber. The reflection from the window during test was deviated by tilt the stage. A pipe heater was used to heat the inside of the temperature chamber. It was fastened close to the bottom of the chamber near where the samples to be placed.

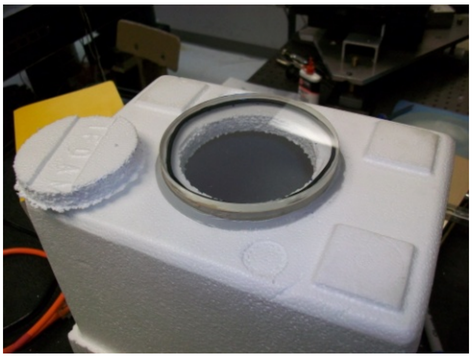

Figure 7: window on the temperature chamber

Figure 8: The pipe heater in the temperature chamber

4 Results

4.1 FEA results

4.1.1Milbond

For Milbond, more adhesive will cause more deflection on the top surface of optics. For certain amount (thickness) of Milbond, the biggest deflection will happen at 60˚C.

4.1.1.1 Top surface deflection

In my analysis, the deflection of top surface is illustrated by expansion difference (vertical displacement difference) at the surface. A model is shown as below with 0.4mm (manufacturer recommended) Milbond and roughly 20˚C temperature raise (from 24.85˚C to 45˚C). In Figure 9, the bulge effect of the adhesive at the edge (greatly scaled in plot) can be seen. It is also clear that the glass is bended down by the adhesive. This phenomenon matches the face that adhesive tends to expand more than glass at the free edge. Figure 10 shows the profile of the vertical displacement along radius.

Max 1.755

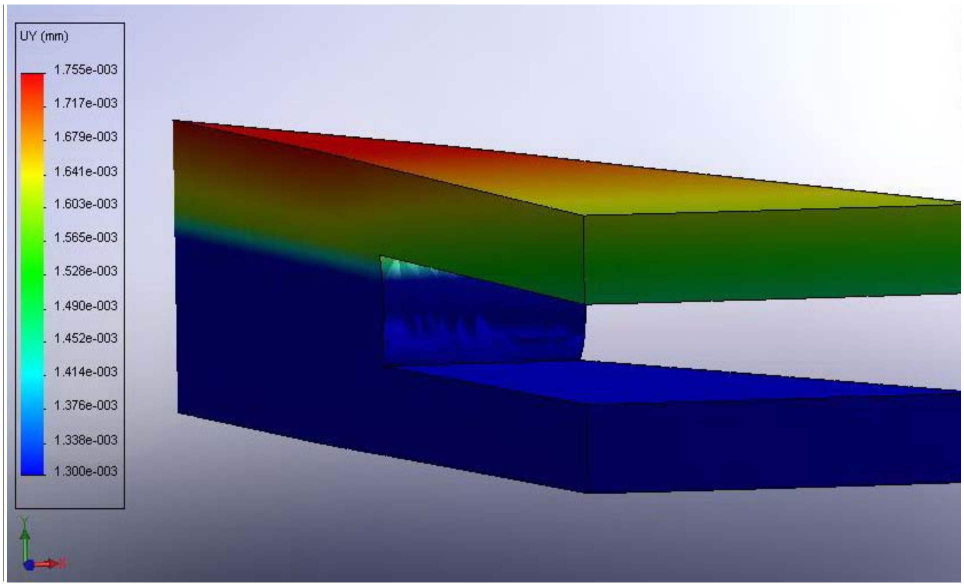

Figure 9: Vertical displacement. The picture shows the sample with 0.4 mm thick Milbond under 24.85˚C to 45˚C temperature change. Minimum value is set such to illustrate the top surface gradient better.

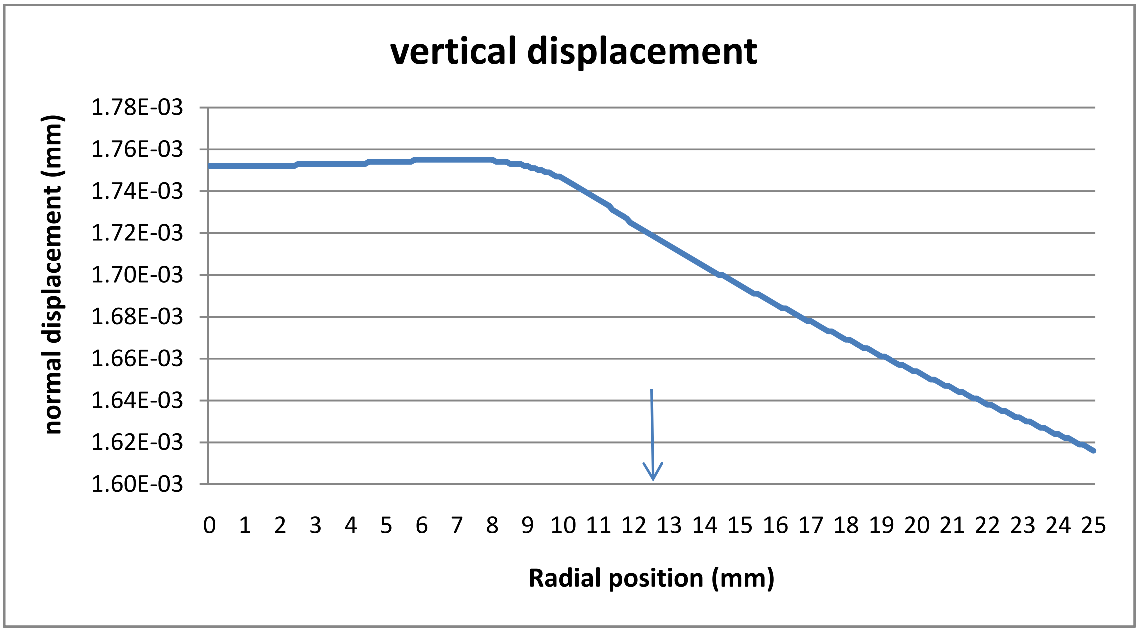

Figure 10: Profile of the top surface deflection. This is the sample with 0.4 mm thick Milbond under 24˚C to 45˚C temperature change. The arrow shows the edge position of the adhesive.

At the center area (the tip of the fan), the displacement is about 1750 nm according to the profile. According to hand calculation, the thickness expansion of the two pieces of glass is 295 nm in total. Because glass has lower CTE, we can assume its expansion is not affected by the bond (which means we can assume the hand calculation equal to the FEA result). Then, the thickness expansion of adhesive in FEA should be 1455 nm, compared with 576 nm by hand calculation. This result matches the effect that the interior adhesive can only expand in one direction rather than three, so there is a factor of nearly three in the expansion in this direction.

One can see from Figure 10 that the bend happens just inside the adhesive free edge. As will be shown later, the bend happens near the area where the largest 1st principle stress locates. This, as expected, is caused by the edge effect of the adhesive (the difference of expansion tendency at the edge area of the adhesive).

As one may notice that the trend of the bending in Figure 10 does not stop at the edge of the 25 mm. As Brian Cuerden indicates, according to some mechanical theory, the glass will tend to bend back to parallel at some place far enough. A model is made to show the effect. See Figure 11. From this figure one can see that the displacement P-V value is greatly decided by the size of the glass.

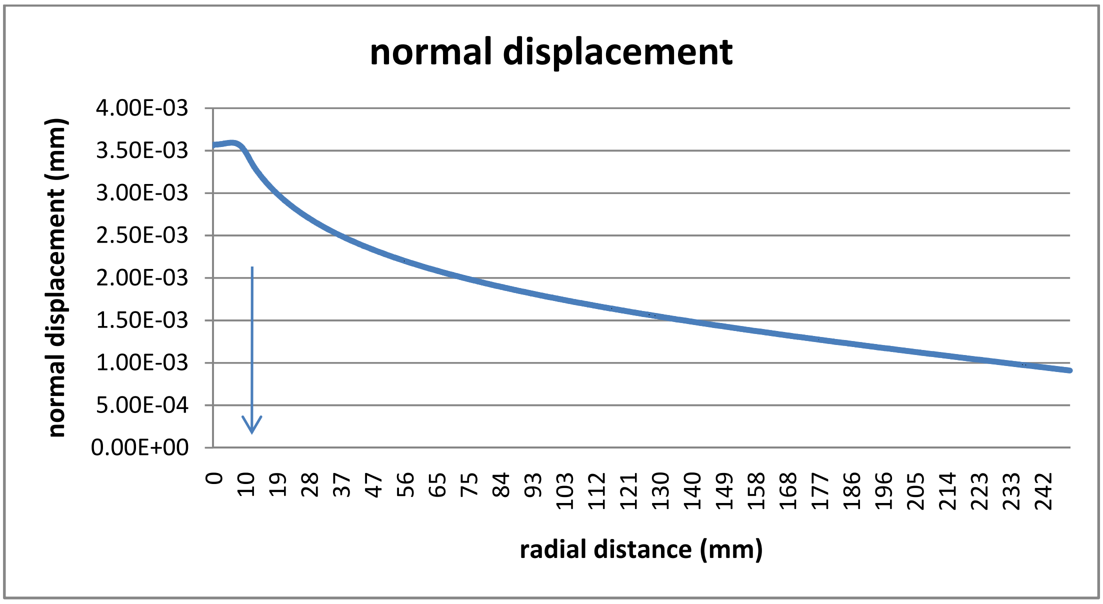

Figure 11: Vertical displacement for large diameter glass. This is the sample with 0.4 mm thick Milbond under 24˚C to 45˚C temperature change. The arrow shows the edge position of the adhesive.

4.1.1.2 Stress Distribution for Milbond: 1st principle in glass & von Mises stress in adhesive

Figure 12 and 13 illustrate the 1st principle stress in the glass. 1st principle stress is the largest normal stress in one element. As glass tends to crack normal to the largest tensile stress, 1st principle stress is the stress causes cracks in glass.

Max 150.9

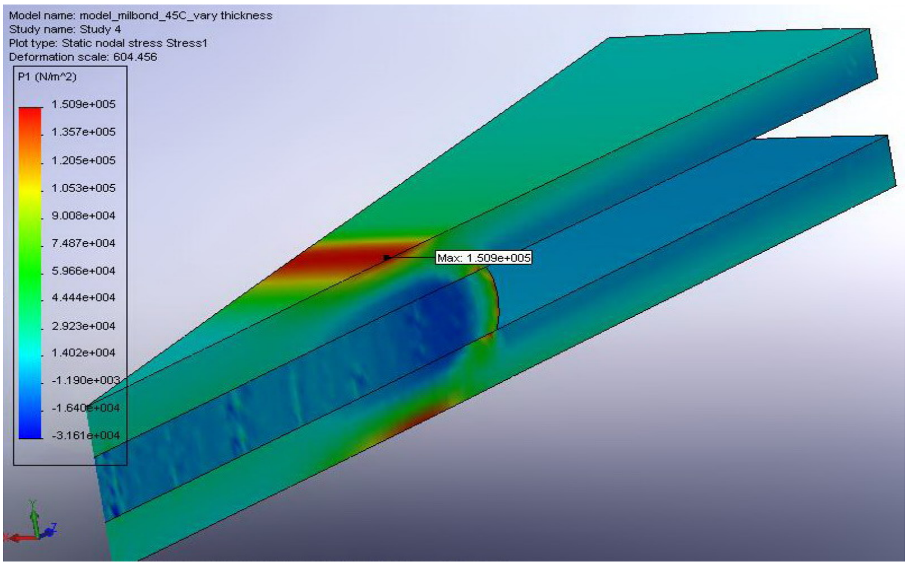

Figure 12: 1st principle stress in glass. This the model with 0.4 mm thick Milbond under 24.85˚C to 45˚C temperature change.

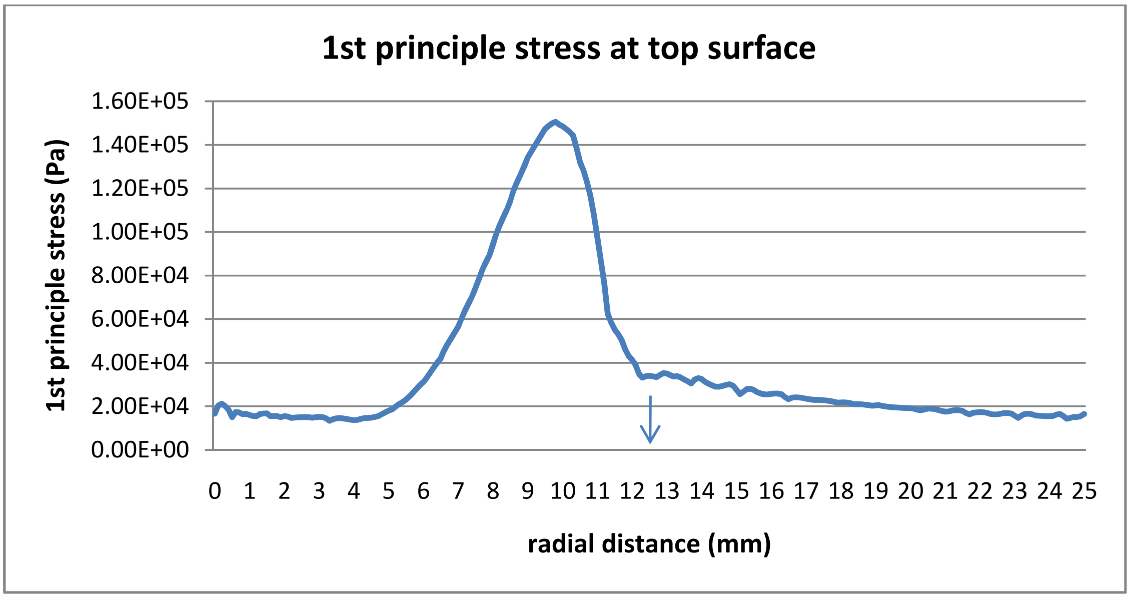

Figure 13: Profile of 1st principle stress at top surface along radius. This the model with 0.4 mm thick Milbond under 24.85˚C to 45˚C temperature change. The arrow shows the position of the free edge of the adhesive.

One can see in Figure 12 that there is highly localized stress at the area where the edge of the adhesive attaches. In the shown case, the stress is small, and will not cause any damage to the glass. There is also some high stress locate at the top surface. This is mainly caused by the bending of the glass by the expand adhesive. Figure 12 shows how the stress at the top surface distributes. One can see that the highest stress occurs just inside the free edge of the adhesive, coincides with the bend shown in Figure 10.

Figure 14 and 15 illustrate the von Mises stress distribution in the adhesive. Von Mises stress (also called equivalent stress) provides adequate information to assess the safety of the design for many ductile materials. It is fully defined by magnitude with stress units without direction. A material starts to yield at a point when the von Mises stress reaches the yield strength of the material.

Max 203.8 KPa

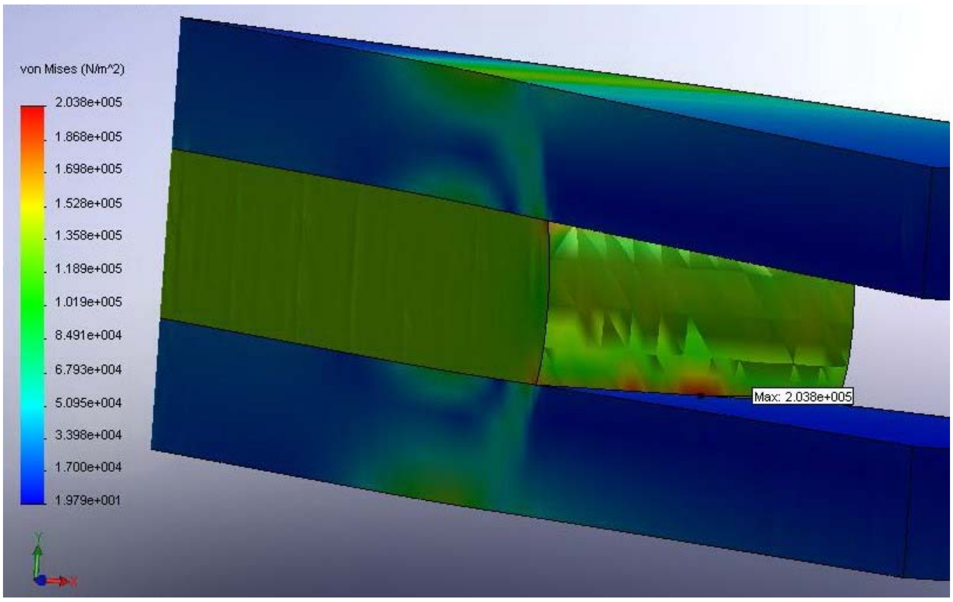

Figure 14: Von Mises stress in adhesive. This the model with 0.4 mm thick Milbond under 24.85˚C to 45˚C temperature change.

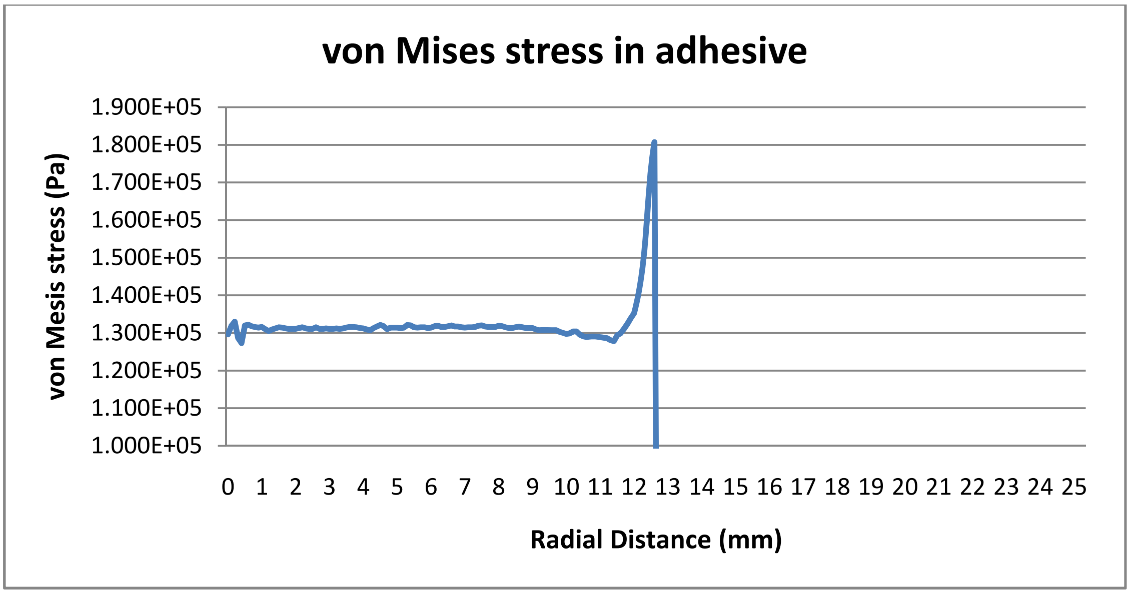

Figure 15: Profile of von Mises stress in adhesive along radius (z axis in Figure 13). This the model with 0.4 mm thick Milbond under 24.85˚C to 45˚C temperature change. For easier compare, the horizontal axis is drawn to 25mm. The radius of adhesive is only 12.5mm where the stress drops to zero in the plot.

As Figure 14 shows, the highest von Mises stress concentrates at the right corner of the bond where the free edge of the adhesive connects with the glass. This is not difficult to understand. The most outside adhesive tends to expand most, which means the most expansion difference tendency with the glass. As the tendency is impeded by the glass (the adhesive and the glass is bonded together), the largest tendency introduce the largest stress.

The largest von Mises stress shown in Figure 14 is 0.2 MPa, which is much smaller than the 5.6 MPa tensile strength of Milbond. If the mesh of the model is fined down, the maximum stress can go up to 20 MPa (actually it is a singularity at the corner). This high stress will cause the yield of the local adhesive. But this phenomenon will not affect the reliability of the current analysis very much, since the high stress is highly localized and can only propagate a tiny distance.

4.1.1.3 Deflection – Temperature Relationship for Milbond

Now, let's see how the top surface deflection changes with temperature. What is shown below is a model with 25 mm diameter and 0.4 mm Milbond. The temperature change is from 24.85˚C to 70˚C. The result is shown in Figure 16.

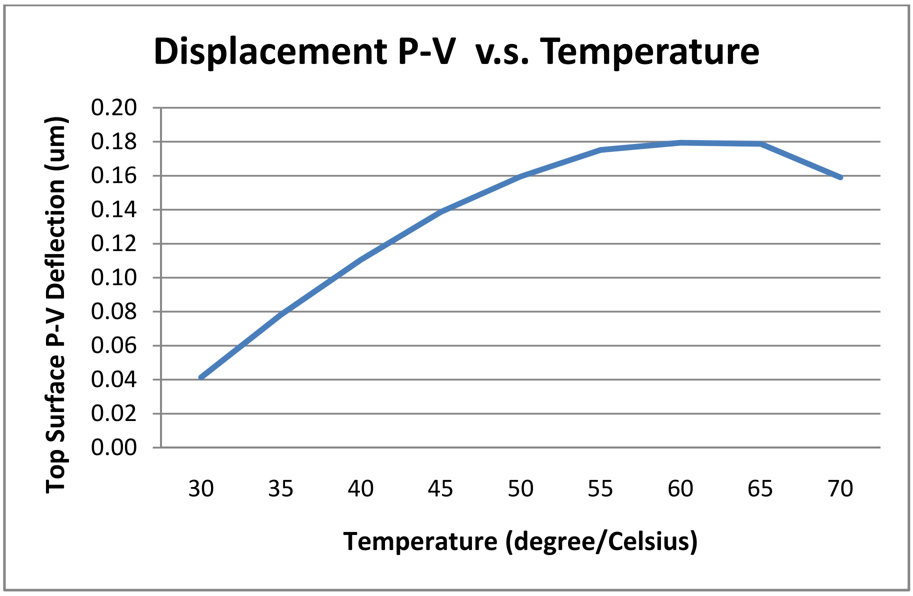

Figure 16: Top surface P-V vs. temperature. It is a model of Milbond with 25 mm diameter and 0.4 mm thickness.

The deflection is defined as P-V displacement in Figure 16. The value of the vertical axis is the difference between max and min value in top surface vertical displacement (refer to Figure 10). One can see that the curve in Figure 16 goes up with temperature. It reaches the highest point of 0.18 um at 60˚C, and then drops as temperature keeps on rising. This means that the deflection of the top surface will not always increase with temperature. This is because the Young's modulus (E) of Milbond decreases as the temperature rise. The Young's modulus of Milbond looks like Figure 17:

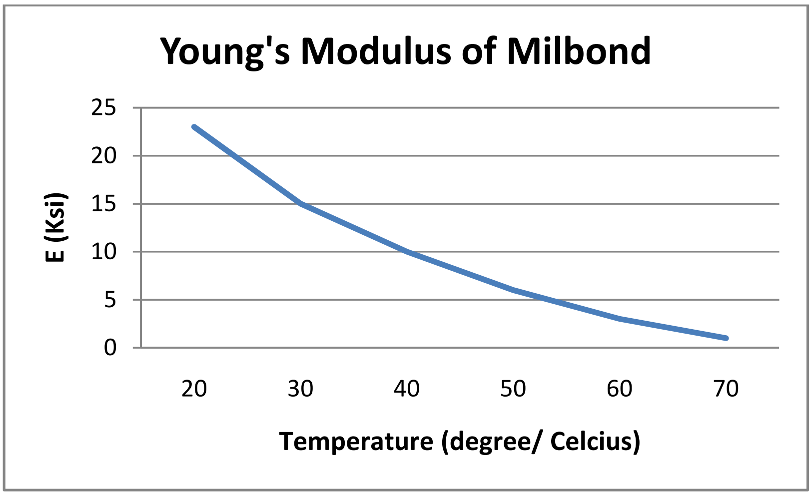

Figure 17: Young's Modulus of Milbond. This figure is drawn according to the Milbond data sheet.

This curve is estimated according to the plot and data in the Milbond data sheet (see appendix). It is clear that the Young's modulus of Milbond decreases quickly with rising temperature. The decrease in the modulus cancels the effect of thermal expansion in producing stress on the glass.

4.1.1.4 Deflection - Adhesive Thickness Relationship for Milbond

In this section, the top surface deflection (P-V vertical displacement) is related to the thickness of the adhesive. The sample has 25 mm diameter Milbond. The temperature change is from 24.85˚C to 45˚C. The thickness of the bond varies from 0.1 mm to 0.9 mm (which is really large for this kind of adhesive). The result is shown in Figure 18:

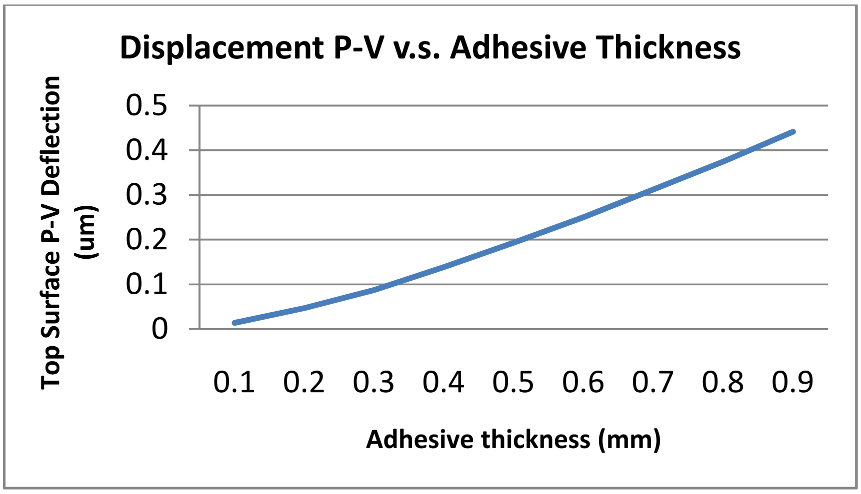

Figure 18: Top surface P-V displacement vs. adhesive thickness.

The Deflection (vertical displacement P-V) increases with the thickness. The curve is almost linear. One can see that the more adhesive used the bigger effect one will get. The increased thickness has more space to give, so the effect of the "free edge" is bigger, which produce larger deflection in the glass. This effect can also be seen by look at the max displacement position change. See Figure 19.

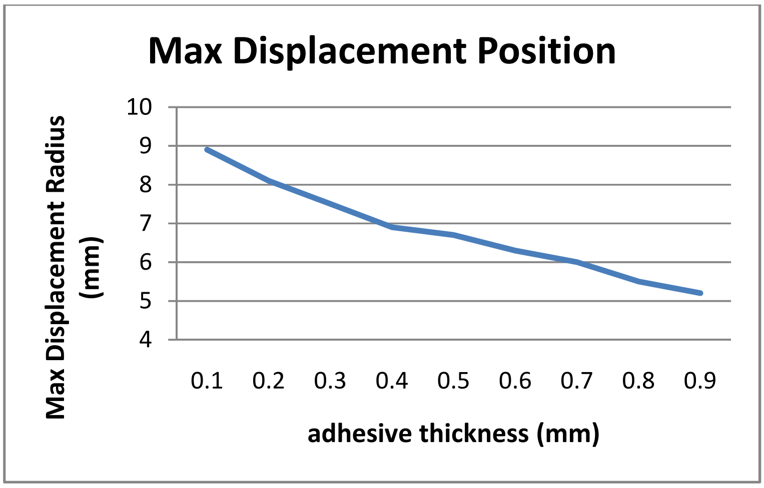

Figure 19: Max vertical displacement position change with thickness

The max displacement is where the bending happens, as shown in Figure 10. It is clear that the bend "point" (actually a circle) can move really close to the center as the thickness increases. This, from another aspect, reflects the increase of edge effect influence with rising thickness.

4.1.2 GE RTV 566

For RTV 566, the thermal deflection is proportion to temperature. For 25 mm diameter bond and 20˚C temperature rising, 3 mm thickness will cause the biggest deflection.

4.1.2.1 Top surface deflection

In this analysis, the adhesive in the model is RTV 566. To compare with Milbond, the thickness is also 0.4mm and the temperature change is also from 24.85˚C to 45˚C. Figure 20 shows the profile of the top surface vertical displacement.

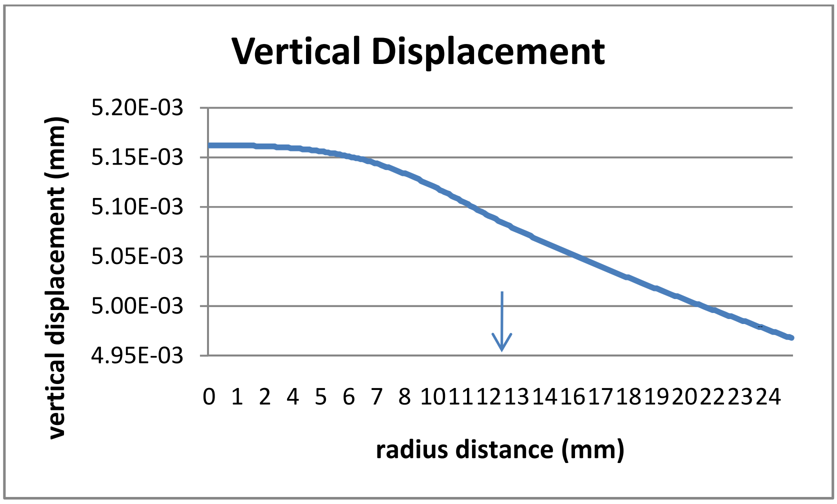

Figure 20: Vertical displacement. This is the sample with 0.4 mm thick RTV 566 under 24˚C to 45˚C temperature change. The arrow shows the edge position of the adhesive.

As can be seen, the top surface deflection is similar to Figure 10. Because of the CTE of RTV 566 (23.3e-5/K) is about three times to the one of Milbond (7.2e-5/K), the absolute displacement in Figure 20 is about three time of that in Figure 10. Since RTV 566 has lower Young's modulus (610 Psi compared to Milbond about 8 Ksi at 45˚C), the "edge effect" is shown closer to the center area. This makes the P-V displacement larger than the Milbond model. But one can see that the bending is flatter in Figure 20.

4.1.1.2 Stress Distribution for RTV 566: 1st principle in glass & von Mises stress in adhesive

The 1st principle stress in glass is shown in Figure 21. The stress is much smaller than the stress in the Milbond model.

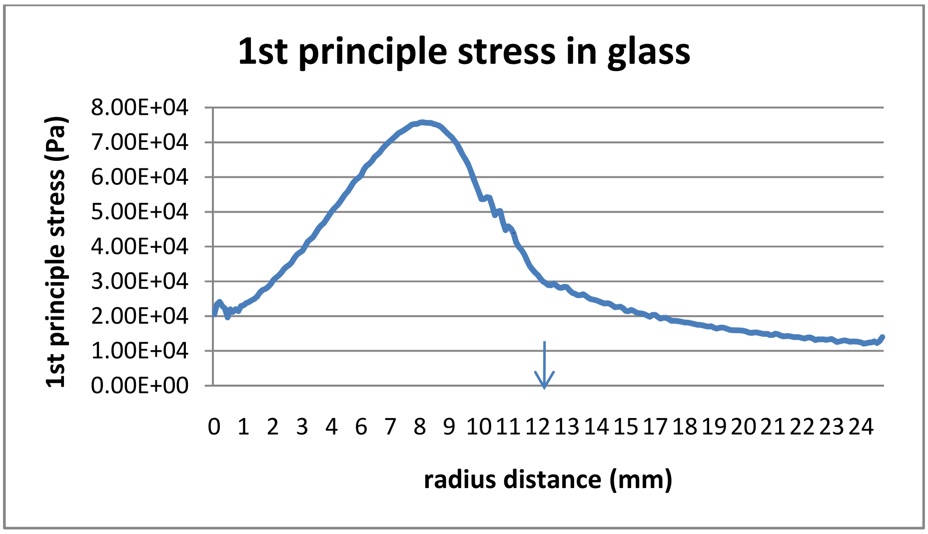

Figure 21:1st principle stress in glass. This is the sample with 0.4 mm thick RTV 566 under 24˚C to 45˚C temperature change. The arrow shows the edge position of the adhesive.

The von Mises stress in the RTV is shown in Figure 22. This is also smaller than Milbond. The maximum value is much smaller than the tensile strength of RTV 566 (5.6e+6 Pa).

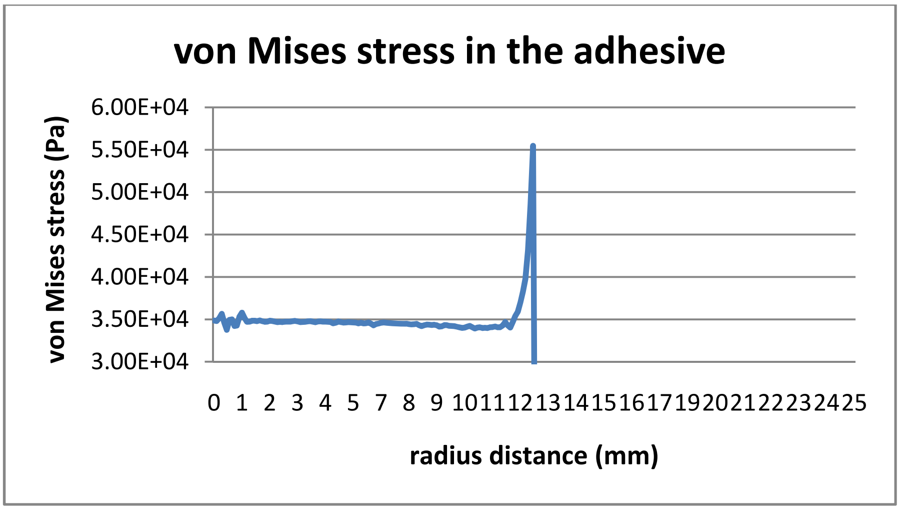

Figure 22: von Mises stress in RTV 566. This is the sample with 0.4 mm thick RTV 566 under 24˚C to 45˚C temperature change.

4.1.2.3 Deflection – Temperature Relationship for RTV 566

A model with 25 mm diameter and 2.0 mm (a reasonable thickness for RTV) RTV 566 is shown below. The temperature change is from 24.85˚C to 70˚C. The result is shown in Figure 23.

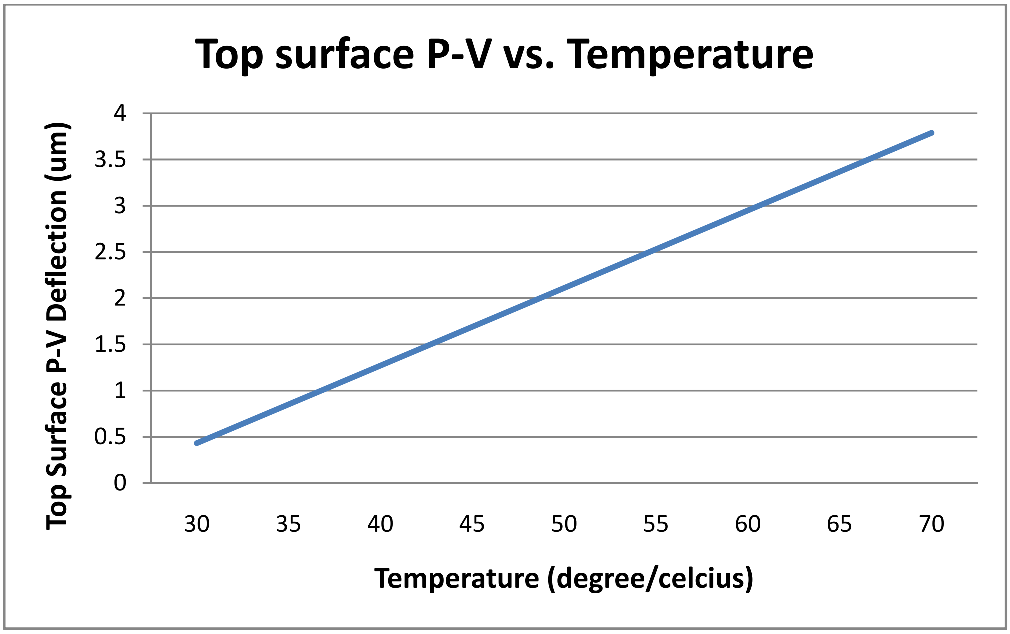

Figure 23: Top surface P-V vs. temperature. It is a model of RTV 566 with 25 mm diameter and 2.0 mm thickness.

The deflection is defined as P-V vertical displacement. The deflection is large due to the properties of RTV and the bigger thickness. Since all the data of the RTV 566 properties (like CTE and Young's modulus) are single-value, the effect shown on plot is linear.

4.1.1.4 Deflection - Adhesive Thickness Relationship for RTV 566

In this section, the sample has 25 mm diameter. The temperature change is from 24.85˚C to 45˚C. The thickness of the bond varies from 0.5 mm to 6 mm (which is reasonable for RTV). The result is shown in Figure 24:

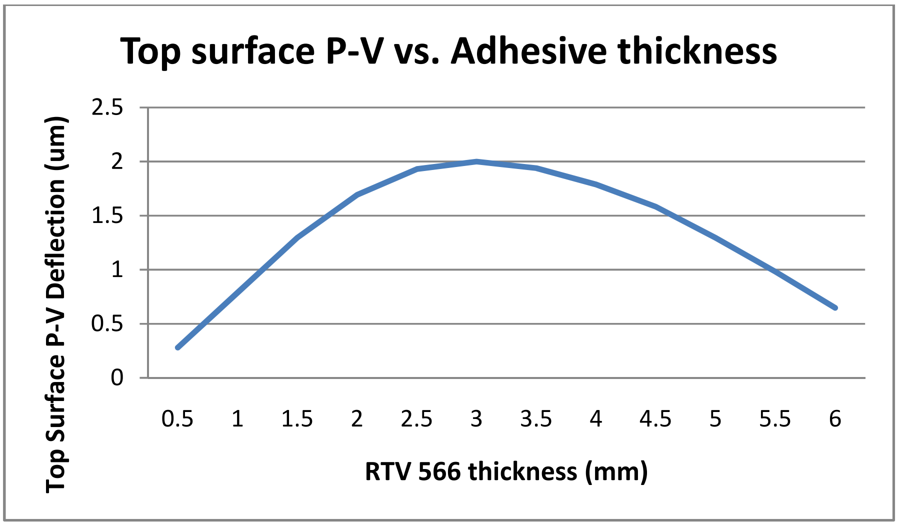

Figure 24: Top surface P-V vertical displacement vs. adhesive thickness. The sample has 25 mm diameter RTV 566. The temperature change is from 24.85˚C to 45˚C.

This is an interesting plot. At small thicknesses, the deflection (vertical displacement P-V) increases with the thickness. The curve is almost linear. But after reaching a peak of 2 um with 3 mm thickness, the deflection goes down when the thickness increased.

To illustrate this effect more clearly, the vertical displacement profile for 3 mm and 6 mm thick RVT are shown as below.

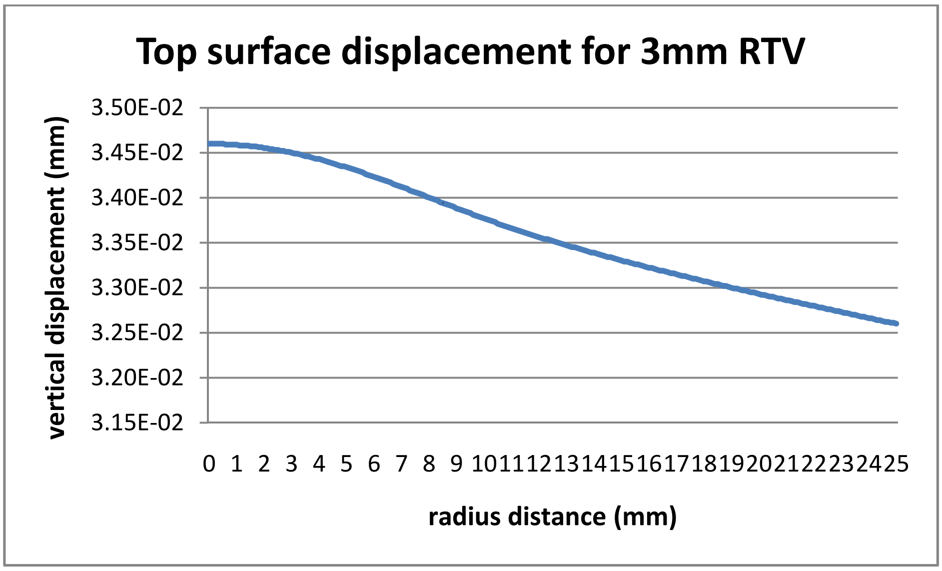

Figure 25: Top surface vertical displacement for 3mm RTV

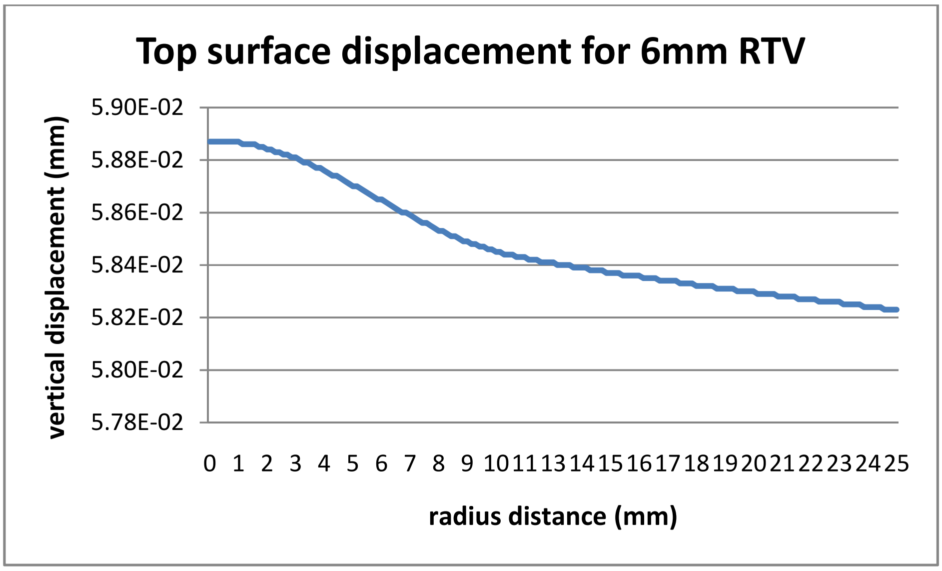

Figure 26: Top surface vertical displacement for 6mm thick RTV

One can see that unlike the plot of 3mm, the profile of 6 mm RTV bends back at 10-11 mm radius. This decreases the P-V displacement value.

The explanation to this is not clear. A possible one is that because the low Young's modulus of the RTV and the concentration of stress to the center, the "bend back to parallel" effect (as mentioned before in 4.1.1.1) shows up trying to bend the glass back to parallel.

4.2 Testing results

Testing for the samples proved to be difficult. The bonded windows could not produce a desirable pattern cross the top surface. Only part of the top surface could be measured with interferometer. The reflections from other surfaces were also difficult to deal with. What I did was narrow down the measure mask, to focus on one part of the sample. Adjusting the interferometer and the software (IntelliWave) setting also took a lot of time.

Sample 1 – Milbond 0.4 mm thickness, 35 mm diameter

This measurement was done in a multi-test. Sample 1-3 were put into the thermal chamber together. For each temperature, the chamber was opened; then, the sample to be test was placed in marked position. After close the chamber and waiting the temperature be still again, measurements were taken. The purpose of doing this was to be more effective. During the measurement, the tilt aberrations were removed. For each measurement, stage was adjusted to get the best measurement.

Figure 27-29 show the measure result of sample 1. Figure 27 shows the sample top surface condition at room temperature. The most left picture is a modulus fringe pattern; in the middle is an OPD map computed by IntelliWave; the most right table is the aberration data of the OPD map. In the modulus picture on can see the outline of the glass. The bond was a little bit deviate downwards from the center. So the mask (the blue ring) was fulfilled mostly by the bond area. Figure 28 shows the surface condition at 46˚C.The same mask as in Figure 27was used. Figure 29 shows the subtract result of two above OPD map.

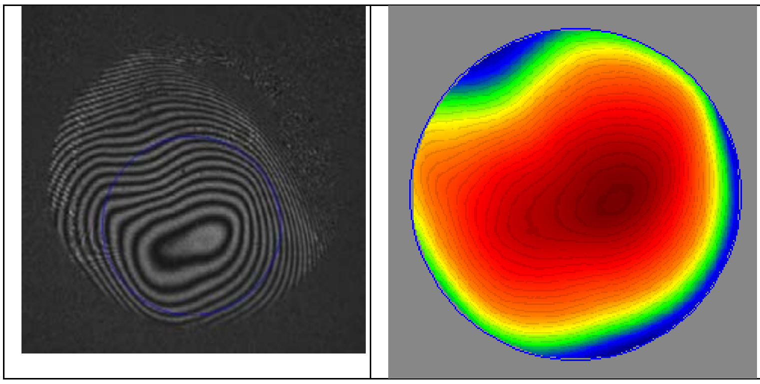

	UofA	WAVES	QC	Ord	RMS
1	Piston	1.7902		0	
2	X Tilt	~~-0.0202~~		1	0.3323
3	Y Tilt	~~-0.0063~~		1	
4	Focus	-1.3275		1	
5	X Astig	0.3192		2	0.1784
6	Y Astig	-0.4750		2	
7	X Coma	-0.3891		2	
8	Y Coma	-0.1733		2	
9	Spherical	0.0147		2	
10	X Trefoil	-0.2613		3	0.0981
11	Y Trefoil.	0.0056		3	

Figure 27: Sample 1 at 24˚C. The blue ring in the most left picture is the measure mask.

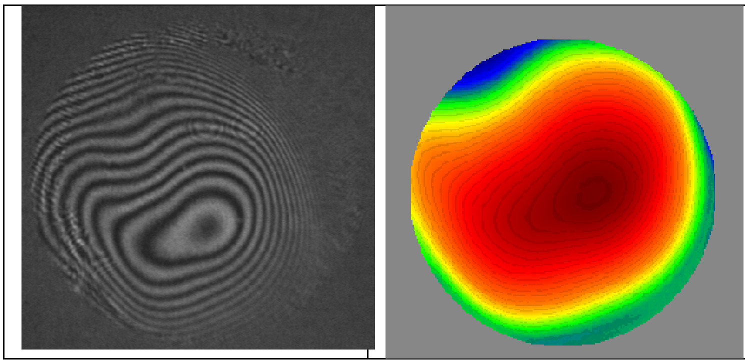

	UofA	WAVES	QC	Ord	RMS
1	Piston	5.1042		0	
2	X Tilt	29.4178		1	4.5898
3	Y Tilt	11.2207		1	
4	Focus	9.3787		1	
5	X Astig	-9.1642		2	8.3234
6	Y Astig	12.2712		2	
7	X Coma	-14.7758		2	
8	Y Coma	1.9032		2	
9	Spherical	-1.5820		2	
10	X Trefoil	-6.2245		3	4.6055
11	Y Trefoil.	-0.2174		3	

Figure 28: Sample 1 at 46˚C

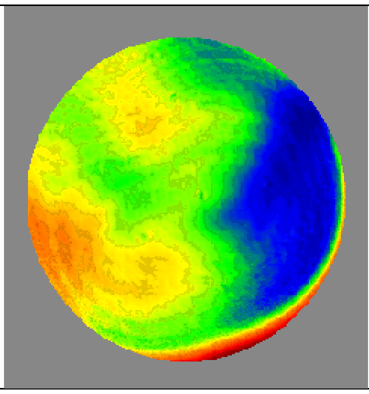

	UofA	WAVES	QC	Ord	RMS
1	Piston	51.6582		0	
2	X Tilt	25.1388		1	11.1142
3	Y Tilt	26.3551		1	
4	Focus	49.0486		1	
5	X Astig	-23.0596		2	11.0230
6	Y Astig	2.8697		2	
7	X Coma	-25.2061		2	
8	Y Coma	56.1850		2	
9	Spherical	-5.5512		2	
10	X Trefoil	-21.3125		3	19.1201
11	Y Trefoil.	33.2582		3	

Figure 29: OPD map of the difference between two temperatures

The result is quite different with expectation. In the left picture in Figure 29, the red strip at the bottom is probably cause by the movement of the sample in two measurements. The blue area indicates a bend at the right side of the mask, where is actually mainly occupied by bond area. It is expected to have some bending shown at the bottom, which is not the case as Figure 29 shows.

By comparing the "Focus" aberration in Figure 27 and 28, one can see that there is a bump introduced by heating. But the difference between the two (10 waves, λ=632.8 nm) is way too much than FEA result.

There still are some problems in verifying and interpreting the results.

Sample 2 – Milbond 0.19 mm thickness, 30 mm diameter

Sample 2 had the similar condition with sample 1. Figure 30-32 show the result of sample 2.

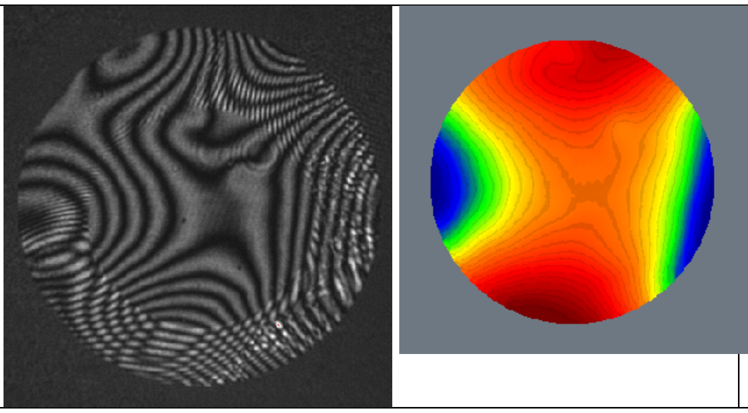

	UofA	WAVES	QC	Ord	RMS
1	Piston	-34.2826		0	
2	X Tilt	~~2.7840~~		1	5.9663
3	Y Tilt	~~-17.5585~~		1	
4	Focus	-31.6684		1	
5	X Astig	26.0757		2	8.8447
6	Y Astig	18.7925		2	
7	X Coma	10.4718		2	
8	Y Coma	-30.7590		2	
9	Spherical	22.9947		2	
10	X Trefoil	-10.3086		3	13.8497
11	Y Trefoil.	-21.3618		3	

Figure 30: Sample 2 at 24˚C

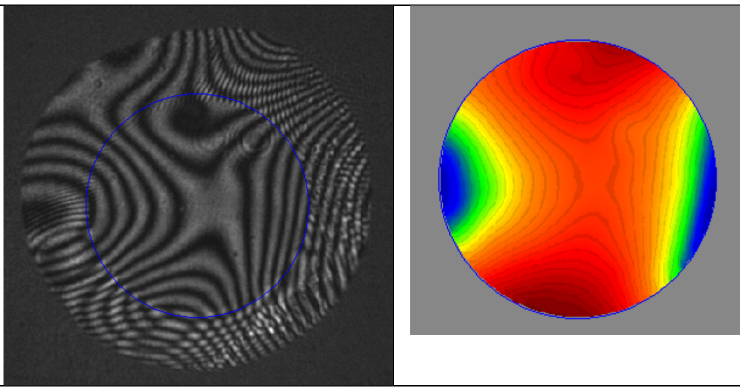

	UofA	WAVES	QC	Ord	RMS
1	Piston	2.1203		0	
2	X Tilt	~~-0.0155~~		1	0.7954
3	Y Tilt	~~0.0054~~		1	
4	Focus	-0.1985		1	
5	X Astig	-1.8890		2	0.1680
6	Y Astig	-0.3304		2	
7	X Coma	-0.2792		2	
8	Y Coma	0.0276		2	
9	Spherical	-0.0259		2	
10	X Trefoil	0.2352		3	0.0893
11	Y Trefoil.	-0.2698		3	

Figure 31: Sample 2 at 46˚C

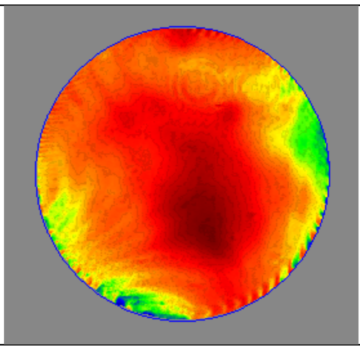

	UofA	WAVES	QC	Ord	RMS
1	Piston	0.2972		0	
2	X Tilt	~~-0.0007~~		1	0.0613
3	Y Tilt	~~-0.0026~~		1	
4	Focus	-0.1174		1	
5	X Astig	-0.0574		2	0.0373
6	Y Astig	0.0732		2	
7	X Coma	-0.0400		2	
8	Y Coma	-0.0609		2	
9	Spherical	0.0386		2	
10	X Trefoil	-0.0422		3	0.0297
11	Y Trefoil.	0.0119		3	

Figure 32: OPD map of the difference between two temperatures

The mask is mainly filled with bond area in this test, as can be seen in the modulus fringe patterns. According to FEA, the surface should not have much difference at this area. At this point, the aberrations shown in Figure 32 seem make sense. But the aberrations, especially the focus term, in Figure 30 seem ridicules.

Sample 3 – Milbond 0.6 mm thickness, 35 mm diameter

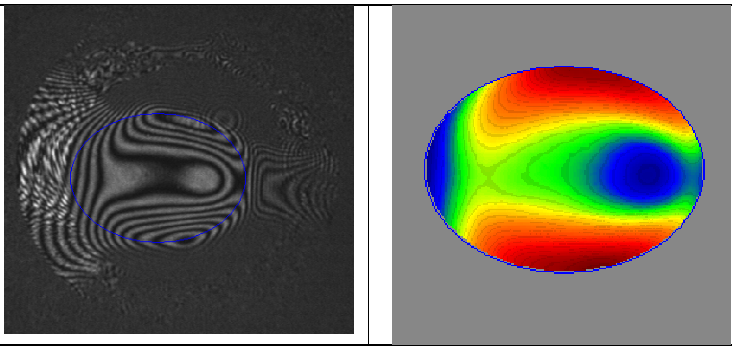

	UofA	WAVES	QC	Ord	RMS
1	Piston	1.3112		0	
2	X Tilt	~~0.2249~~		1	0.7950
3	Y Tilt	~~0.2740~~		1	
4	Focus	-0.1094		1	
5	X Astig	-0.8272		2	0.4966
6	Y Astig	-0.3209		2	
7	X Coma	0.5457		2	
8	Y Coma	0.3195		2	
9	Spherical	-1.1208		2	
10	X Trefoil	-0.4437		3	0.2112
11	Y Trefoil.	-0.0566		3	

Figure 33: Sample 3 at 24˚C

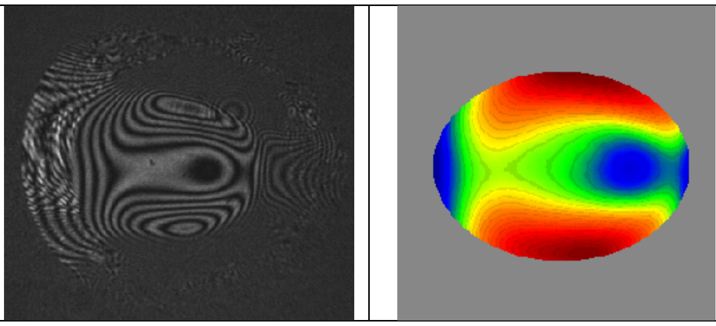

	UofA	WAVES	QC	Ord	RMS
1	Piston	-34.9635		0	
2	X Tilt	~~-40.6128~~		1	9.5105
3	Y Tilt	~~-76.9896~~		1	
4	Focus	-38.6238		1	
5	X Astig	59.8562		2	25.4300
6	Y Astig	-30.9481		2	
7	X Coma	15.2223		2	
8	Y Coma	35.9584		2	
9	Spherical	55.8331		2	
10	X Trefoil	3.6024		3	12.6027
11	Y Trefoil	128.5998		3	

Figure 34: Sample 3 at 46˚C

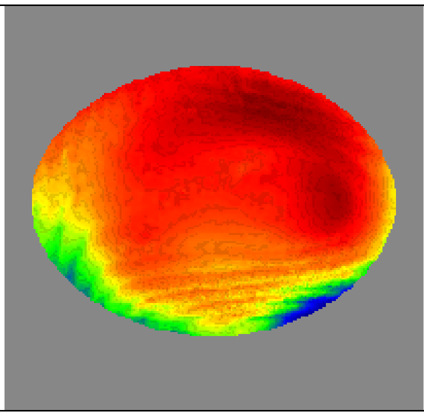

	UofA	WAVES	QC	Ord	RMS
1	Piston	-3.8554		0	
2	X Tilt	~~-53.5820~~		1	5.8770
3	Y Tilt	~~-14.1317~~		1	
4	Focus	1.7525		1	
5	X Astig	3.1173		2	14.6872
6	Y Astig	-0.8534		2	
7	X Coma	45.9612		2	
8	Y Coma	9.1310		2	
9	Spherical	1.3583		2	
10	X Trefoil	-5.9938		3	7.9690
11	Y Trefoil.	0.4731		3	
12	X Astig	11.3719		3	

Figure 35: OPD map of the difference between two temperatures

Sample 4 – Milbond 0.4 mm thickness, 10 mm diameter

Sample 4 was found failed one day during late this semester. Seems the adhesive did not have enough interaction with one of the glass surface. It is probably that inadequate press was exerted on the sample when the bond was made.

After this, the remained adhesive was examined. When the adhesive were prepared and applied, the remaining adhesive was kept for later examine. After the failure of Sample 4, the adhesive was cut apart to be examined. Both the Milbond and RTV 566 looked in right condition. So the failure of sample 4 should not be caused by the problem of the adhesive; and should not influent other samples. Figure 36 shows the section of remained adhesive.

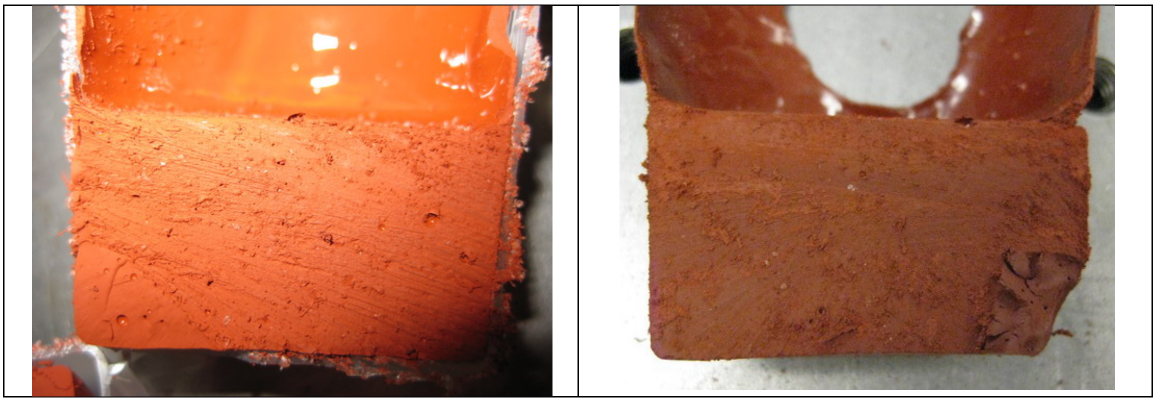

Figure 36: The section of remained adhesive. RTV 566 is on the left while Milbond on the right

Sample 5 – RTV 566 0.75 mm thickness, 40 mm diameter

Sample 5 and 6 were tested together in the similar way with sample 1-3. Figure 37-39 show the result of sample 5.

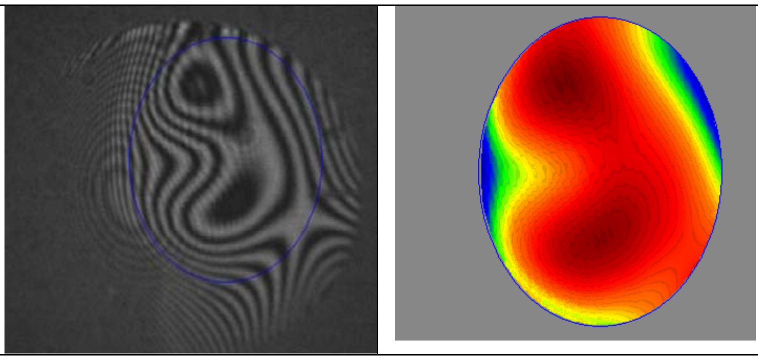

	UofA	WAVES	QC	Ord	RMS
1	Piston	1.5615		0	
2	X Tilt	~~0.2281~~		1	0.5512
3	Y Tilt	~~0.1541~~		1	
4	Focus	-0.5096		1	
5	X Astig	-0.5832		2	0.4274
6	Y Astig	0.7165		2	
7	X Coma	0.1209		2	
8	Y Coma	0.0295		2	
9	Spherical	0.3303		2	
10	X Trefoil	0.4768		3	0.1721
11	Y Trefoil.	0.6662		3	
12	X Astig	1.0021		3	

Figure 37: Sample 5 at 24˚C

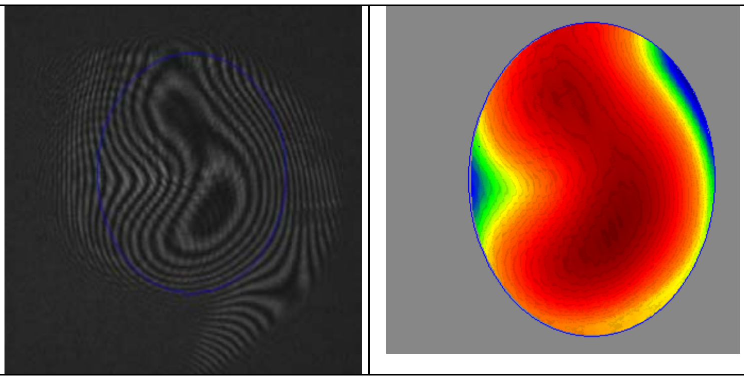

	UofA	WAVES	QC	Ord	RMS
1	Piston	2.5071		0	
2	X Tilt	~~0.5241~~		1	0.8050
3	Y Tilt	~~0.0500~~		1	
4	Focus	-0.8775		1	
5	X Astig	-0.7705		2	0.6822
6	Y Astig	0.6501		2	
7	X Coma	0.4126		2	
8	Y Coma	-0.1594		2	
9	Spherical	0.6907		2	
10	X Trefoil	1.2690		3	0.2328
11	Y Trefoil.	0.3482		3	
12	X Astig	1.5672		3	

Figure 38: Sample 5 at 41˚C

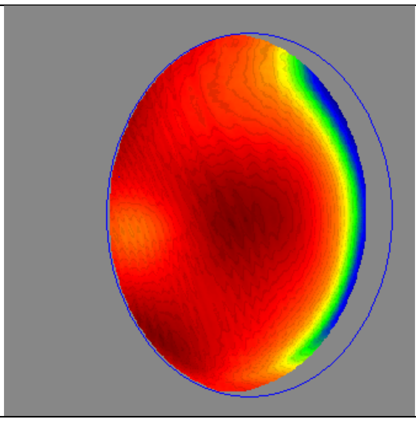

	UofA	WAVES	QC	Ord	RMS
1	Piston	2.2439		0	
2	X Tilt	~~2.2284~~		1	1.3711
3	Y Tilt	~~-0.0777~~		1	
4	Focus	1.6355		1	
5	X Astig	2.8750		2	1.1473
6	Y Astig	-0.2421		2	
7	X Coma	4.4589		2	
8	Y Coma	-0.3316		2	
9	Spherical	2.5184		2	
10	X Trefoil	2.8745		3	0.6920
11	Y Trefoil.	-0.7608		3	
12	X Astig	3.2800		3	

Figure 39: OPD map of the difference between two temperatures

The result does not match the expectation either. The blue strip on the right is probably a tiny mismatch of position of two different OPD map, though their positions were adjusted to get the best result. The expected bending at the top area of mask does not show.

Sample 6 – RTV 566 0.9 mm diameter, 38 mm diameter

Figure 40-42 show the result of testing sample 6. The situation is pretty similar to sample 5. It is difficult to draw some reasonable conclusion.

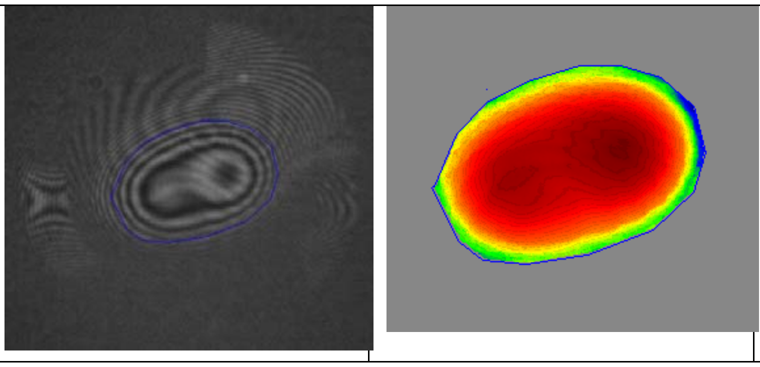

	UofA	WAVES	QC	Ord	RMS
1	Piston	1.4090		0	
2	X Tilt	~~-0.3346~~		1	0.6654
3	Y Tilt	~~-0.7638~~		1	
4	Focus	0.4410		1	
5	X Astig	-1.1714		2	0.6547
6	Y Astig	1.0303		2	
7	X Coma	-0.4836		2	
8	Y Coma	-0.8844		2	
9	Spherical	1.3620		2	
10	X Trefoil	0.5881		3	0.3120
11	Y Trefoil.	0.2845		3	
12	X Astig	-1.9444		3	

Figure 40: Sample 6 at 24˚C

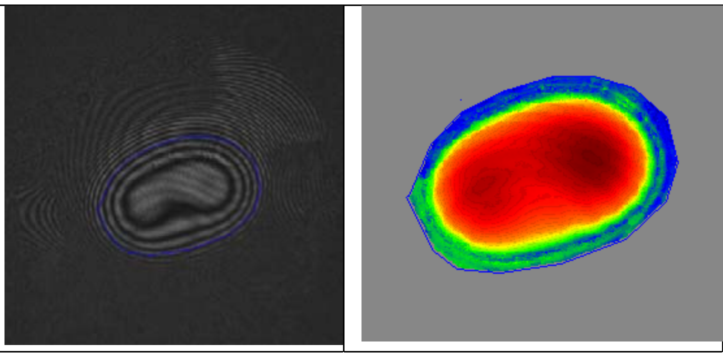

	UofA	WAVES	QC	Ord	RMS
1	Piston	1.0799		0	
2	X Tilt	~~-0.0938~~		1	0.7041
3	Y Tilt	~~-0.0706~~		1	
4	Focus	0.8497		1	
5	X Astig	-1.6625		2	0.6304
6	Y Astig	1.1406		2	
7	X Coma	-0.1841		2	
8	Y Coma	-0.0754		2	
9	Spherical	1.3503		2	
10	X Trefoil	0.1363		3	0.2339
11	Y Trefoil.	-0.0556		3	
12	X Astig	-1.8593		3	

Figure 41: Sample 6 at 41˚C

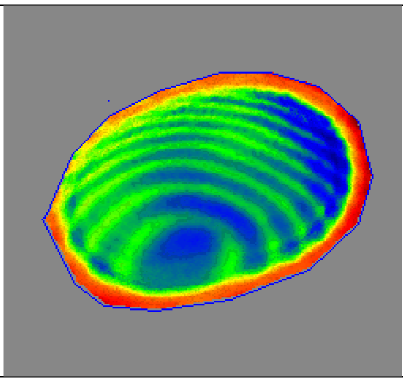

	UofA	WAVES	QC	Ord	RMS
1	Piston	0.4063		0	
2	X Tilt	~~0.3561~~		1	0.3568
3	Y Tilt	~~0.8741~~		1	
4	Focus	0.3946		1	
5	X Astig	-0.4728		2	0.2208
6	Y Astig	0.1483		2	
7	X Coma	0.4815		2	
8	Y Coma	1.0820		2	
9	Spherical	0.0209		2	
10	X Trefoil	-0.6388		3	0.1615
11	Y Trefoil.	-0.3279		3	
12	X Astig	0.0408		3	

Figure 42: OPD map of the difference between two temperatures

Sample 7 – RTV 566 0.75 mm thickness, 15 mm diameter

Sample 7 was treated a little different. It was tested alone, without adjusting the stage between measurements. This measurement was following another measurement. So the temperature was cooled down to 25˚C rather than 24˚C. Figure 43-45 show the results.

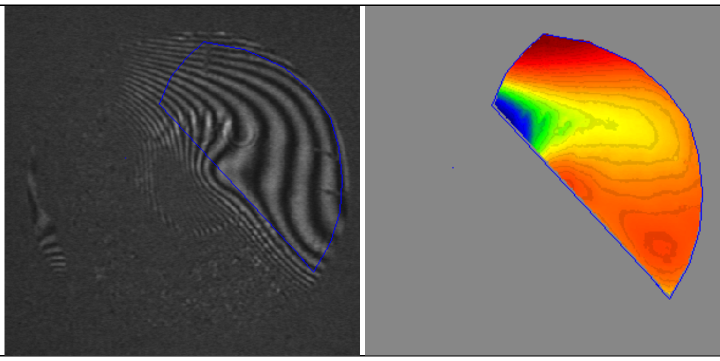

	UofA	WAVES	QC	Ord	RMS
1	Piston	-0.3491		0	
2	X Tilt	~~4.5027~~		1	1.6515
3	Y Tilt	~~-3.6009~~		1	
4	Focus	-2.3951		1	
5	X Astig	-1.2030		2	0.5724
6	Y Astig	4.5180		2	
7	X Coma	2.1546		2	
8	Y Coma	-2.6378		2	
9	Spherical	-0.3791		2	
10	X Trefoil	-1.3229		3	0.2528
11	Y Trefoil	-1.1841		3	

Figure 43: Sample 7 at 25˚C

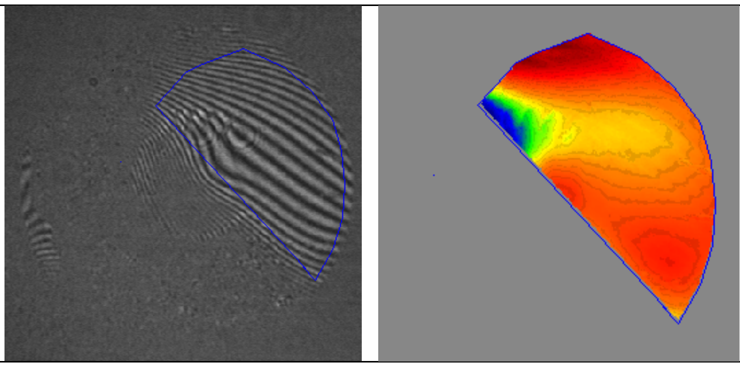

	UofA	WAVES	QC	Ord	RMS
1	Piston	-0.3648		0	
2	X Tilt	~~4.0456~~		1	1.3844
3	Y Tilt	~~-2.8686~~		1	
4	Focus	-2.4131		1	
5	X Astig	-1.7118		2	0.6295
6	Y Astig	3.7242		2	
7	X Coma	2.9175		2	
8	Y Coma	-2.6768		2	
9	Spherical	-1.0813		2	
10	X Trefoil	-0.1471		3	0.2780
11	Y Trefoil.	-1.3407		3	

Figure 44: Sample 7 at 40˚C

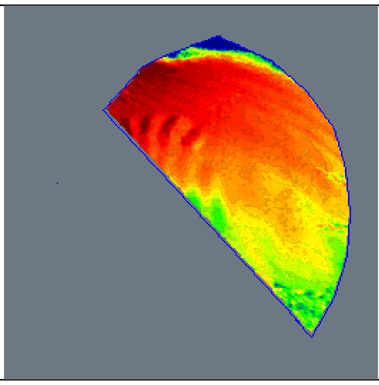

	UofA	WAVES	QC	Ord	RMS
1	Piston	1.4410		0	
2	X Tilt	~~-1.0483~~		1	0.4403
3	Y Tilt	~~1.1590~~		1	
4	Focus	0.2692		1	
5	X Astig	-0.6388		2	0.3935
6	Y Astig	-1.2411		2	
7	X Coma	0.6165		2	
8	Y Coma	-0.0668		2	
9	Spherical	-0.8551		2	
10	X Trefoil	1.5040		3	0.3488
11	Y Trefoil.	-0.0430		3	
12	X Astig	-0.4967		3	

Figure 45: OPD map of the difference between two temperatures

Without adjust the stage, the pattern became very difficult for the software to process. This is because the thermal effect made the surface deflected. So the temperature was only set as high as 40˚C.

Even though the OPD and aberrations chart in Figure 45 is still hard to explain, one can see some difference between the modulus fringe pattern in Figure 44 and 43. In Figure 43, there are roughly four fringes across the radius. That can be interpreted as a two waves tilt (there is a factor of two between wave and surface deflection for reflection test). In Figure 44, there are about ten fringes, which mean five waves tilt. So there are three waves (about 1.9 um) thermal-introduced deflection. This is still much larger than FEA model.

Some improvement should be made to measure better the effect. A better understanding of the interferometer and the software is also needed to obtain better.

5 Conclusion

FEA and experiments are applied to study the thermal effect at the bond area, and how this deflects the optics surface. FEA models show some interesting results while the experiments did not go very well. For Milbond, more adhesive will cause more deflection on the top surface of optics. For certain amount (thickness) of Milbond, the biggest deflection will happen at 60˚C. For RTV 566, the thermal deflection is proportion to temperature. For 25 mm diameter bond and 20˚C temperature rising, 3 mm thickness will cause the biggest deflection.

6 Lessons Learnt

About FEA

From doing FEA in this project, I gain a better understanding that it is your own responsibility to make sure the FEA is right. With computer programs, the analysis can easy go wrong without catching your attention. So keep on asking “if this makes sense” is really important. Using basic equation to do some hand calculation can provide a general sense about whether the computer is doing the right thing. Some basic material properties can be used as judgments, like Roark, Beer and so forth.

If the model is too complicated to do hand calculation, you can use some other simple models to test the program. In my project, I used a “rubber-under-compress” model (provided by Brian Cuerden) to test the COSMOS. When the expected result is given, I would be more confident that the software is able to deal this kind of problem.

Experiences from previous work can also be helpful. Brian Cuerden gave me a lot help in this aspect. His experiences dealing with adhesives and FEA provide good judgments of whether the result is right. For example, he said there should be a singularity at the bond corner when you keep on fine down the mesh. This is a way to test COSMOS.

Time should be spent on reading the help and other materials to understand the software better. There are so many different kinds of options to do different analysis. Make sure you choose the right options to get the desired result. In this aspect, I learnt a lot from talking with Won Hyun Park.

About experiment

In this aspect, I hesitated too much before getting start to try something. My experiment involves cooperation with others, like building the temperature chamber and set up the interferometer. What I was thinking is: “I should wait for Professor Parks to arrange the interferometer.” “Gerard will build the chamber. He needs it too.” But in fact, my test needed much more work because of the poor condition of my glass windows. Counting on others really delayed my own schedule. I realized later that it is no way for others to understand what you need, and myself should take charge in keeping things moving. So what I should do is be more positive to ask for help or communicate with certain people.

Besides, I underestimated the difficulty of my measurement. I gain a better understanding of the saying “everything can go wrong”. So leave some margin when making the schedule is really important.

Reference

1. F. P. Beer, E. R. Johnston, Jr. Mechanics of materials, McGraw-Hill, 1981.
2. W. C. Young, Roark’s Formulas for Stress and Strain, sixth edition, McGraw-Hill
3. Bisplighoff, Mar and Pian, STATICS OF DEFORMABLE SOLIDS, Addison Wesley, Reading MA, 1965

Appendix

Properties of B270

http://www.pgo-online.com/intl/katalog/B270.html

Mechanical Properties

Density	2.55 g/cm^3
Young's modulus E	71.5 kN/mm^2
Poisson's ratio μ	0.219
Torsion modulus G	29.3 kN/mm^2
Knoop hardness HK_{100}	542

Thermal Properties

Coefficient of mean linear thermal expansion (static measurement):

9,4 x 10^{-6}/K (20-300°C)

9,0 x 10^{-6}/K (20-200°C)

8,2 x 10^{-6}/K (20-100°C)

Heat conductivity (W/(m x K):

0,92 (24,5°C)

1,01 (89°C)

1,08 (127°C)

1,15 (167°C)

Thicknesses

Thickness: 0.90mm ±0.10

Properties of Milbond

Approximate Curing Times

Mix Ratio	Room Temperature 25°C (77°F)	Oven Temperature 71°C (160°F)
Epoxy 1:1 (by weight)	7 days	3 hours
Primer 1:1 (by volume)	1 hour (to touch) 24 hours (to dry)	Not Recommended

Specifications

Pot Life @ 25°C...............................Primer- 8 Hours
Epoxy- 30 Min.
Coverage at .015inch (.38mm)..................1322 sq inches
Tensile Shear @ 25°C..........................2,099 psi
- After 60 min @ 70°C......................992 psi
- After 60 min @ -50°C.....................2,561 psi
- After 10 min @ 70°C(100% R.H.)............1,892 psi
(test to failure at .015inch bond layer thickness, all failures cohesive, thinner bond layers yield higher results.)

Modulus of Elasticity @
-50°C....................................85,900 psi
+20°C....................................23,000 psi
+70°C....................................1,070 psi
(2inch long specimens were used, 5 specimens per test, and the crosshead speed was .2"/min)

Mechanical Shock @
-40°C....................................250-400G^s
+20°C....................................250-400G^s
+70°C....................................250-400G^s
(Shock pulses were approximately half sinewave; 1.5 millisecond duration.)

Linear Coefficient Of Expansion
From (+20°C) - (-54°C)....................6.2×10^{-5}/°C
From (+20°C) - (+70°C)....................7.2×10^{-5}/°C
(2inch long (50mm) substrates were used, 2 substrates per test.)

Outgassing TML (Total Mass Loss)..............0.98%
CVCM (ASTM E595)..............................0.03%
(Collected Volatile Condensable Material)
Thermal Conductivity........................300-350 x 10^{-5} cal/(sec)(sq.cm)(°C)(cm)
Specific Heat @

```
   40°C.......................................3 cal/(gm)(°C)
   60°C.......................................35 cal/(gm)(°C)
   80°C.......................................48 cal/(gm)(°C)
Specific Gravities
   Primer Resin...............................1.21
   Primer Curing Agent........................0.82
   Adhesive Part "A" 34.......................1.769
   Adhesive Part "B" 34.......................0.944
   Mixed Adhesive (1:1 Ratio).................1.23
Shelf Life at 22°C............................1 year
```

Youngs Modulus v Temperature

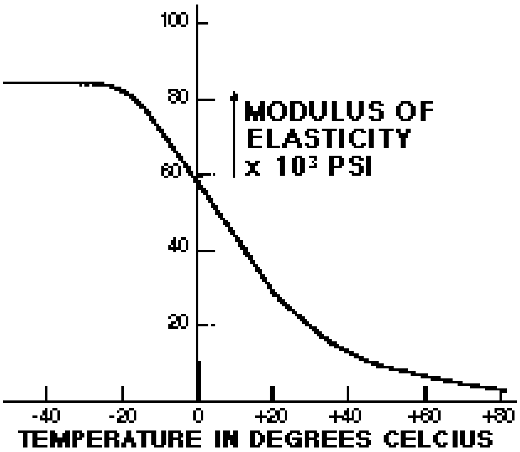

Properties of RTV 566

Density	1510 Kg/m^3
Glass Transition temperature	-105 deg. C.
Young's Modulus	4.2E6N/m^2
Poisson Ratio	0.40 at -100 deg. C; 0.45 at +20 to 200 deg C.
Ultimate Tensile Strength	5.6E6 Pa
Thermal Expansion Coefficient	233E-6/K (-125 to +200)
Durometer	60 (Shore A)
Thermal Conductivity	29 W/mK
Working time	1 Hr. (typical)
Out-gassing %TML	0.11
Cure	>24-hr. full cure is 7 days at ambient
Out-gassing %CVCM	0.01
Tensile Strength	>925 PSI
Viscosity of mix	2E5 CPS
Lap Shear to Al	>500 PSI

BK7 matching oil

CARGILLE
BK-7 MATCHING LIQUID CODE 11510
n (5893 Å) 25 °C = 1.5167
TYPICAL CHARACTERISTICS

COMPOSITION	Phthalate Esters and Chlorinated Aliphatic Hydrocarbons
APPEARANCE	Colorless to Slightly Yellow Liquid
INDEX CHANGE RATE BY EVAPORATION	Very Low : 0.00000 expected, exposed
surface area to volume ratio of 0.2 cm^2 / cc @ 25 °C for 37 days.	
ODOR	Very Slight
COLOR STABILITY	In Sun: may slightly darken after 1 year; very slightly more after 6 years
POUR POINT °C	- 10
BOILING POINT °C @ 760mm Hg	Decomposes
FLASH POINT °C COC	Decomposes at 160 °C
DENSITY g / cc @ 25 °C	1.334
DENSITY TEMP. COEFFICIENT g / cc / °C	-0.0010
COEF. OF THERM. EXP. cc / cc / °C	0.0007
VISCOSITY centistokes @ 25 °C	1,250 , (ca. 2,910 @ 15 °C, 650 @ 35 °C)

SOLUBLE : Acetone, Carbon Tetrachloride, Ethanol, Ethyl Ether, Heptane, Methylene Chloride, Naphtha, Toluene, Turpentine, Xylene

INSOLUBLE : Water

COMPATIBLE 10 month immersion @ 25 °C : Acrylic, Cellulose Acetate, Epoxy, Mylar, Nylon, Polyester, Polyethylene, Polypropylene, Polyurethane, Polyvinyl Chloride, Phenolic, Teflon, Silicone and Fluorosilicone Rubber, Latex Rubber; Aluminum, Copper, Brass, Steel; (tests done on one example of each).

INCOMPATIBLE: Polycarbonate, Polystyrene, Neoprene Rubber and Tygon

TOXICITY........ Low (request MSDS)

CAUCHY EQUATION: refractive index as a function of wavelength at 25 °C

W = wavelength in angstroms (Å)

$$n(W) = 1.502787 + (455872.4) / W^2 + (9.844856E+11) / W^4$$

SOURCE OR SPECTRAL LINE	WAVELENGTH (angstroms)	REFRACTIVE INDEX @ 25 °C Liquid	BK-7	% TRANSMITTANCE 0.1 mm	1 mm	1 cm
near UV cut off	3100	1.561	1.549	97	75	6
i (Hg)	3650	1.543	1.536	100	96	70
h (Hg)	4047	1.5343	1.5302	100	99	91
F' (Cd)	4800	1.5244	1.5228	100	100	98
F (H)	4861	1.5238	1.5224	100	100	99
e (Hg)	5461	1.5192	1.5187	100	100	100
D (Na: D1, D2 mean)	5893	1.5167	1.5167	100	100	100
HeNe laser	6328	1.5148	1.5151	100	100	100
C' (Cd)	6439	1.5144	1.5147	100	100	100
C (H)	6563	1.5139	1.5143	100	100	100
Ruby laser	6943	1.5127	1.5132	100	100	100
GaAs laser	8400	1.5094	1.5100	100	100	99
Nd: YAG laser	10648	1.507	1.507	100	100	98
Diode	13000	1.506	1.504	100	100	96
Diode	15500	1.505	1.501	100	99	90

$n_F - n_C$ = 0.0099

Abbe ν_D : $(n_D-1) / (n_F-n_C)$ = 52.0

Temp. Coef.: dn_D / dt 15-35 °C = -0.000393

CARGILLE LABORATORIES
55 Commerce Road, Cedar Grove, NJ 07009-1289 U.S.A.
Phone: 973-239-6633 / Fax: 973-239-6096 / Email: Cargillelabs@aol.com